A Novel Spatial Autocorrelation Model of Shadow Fading in Urban Macro Environments

Yu Zhang*†, Jianhua Zhang†, Di Dong†, Xin Nie*, Guangyi Liu‡ and Ping Zhang*
* Key Lab. of Universal Wireless Communications (Beijing Univ. of Posts and Telecom.), Ministry of Education, China
Email: {zhangyu, niexin}@mail.wtilabs.cn, pzhang@bupt.edu.cn
† Wireless Technology Innovation Institute, Beijing Univ. of Posts and Telecom., P.O. Box #92, China, 100876
Email: jhzhang@bupt.edu.cn, dongdi@mail.wtilabs.cn
‡ Research Institute of China Mobile Communications Corporation, Beijing, China, 100053
Email: liuguangyi@chinamobile.com

***Abstract*—In this paper, we propose a novel spatial autocorrelation model of the shadow fading process in urban macro environments. The proposed model is based on the empirical results obtained from extensive wideband radio channel measurement campaigns at 2.35 GHz in an urban area of a typical medium-sized Chinese city. The shadow fading component was extracted assuming a single-slope log-distance path loss model. The consistency with the level crossing theory of Gaussian processes is achieved by an implicit constraint on the parameters of the model. The proposed model gives a better fit to the empirical results in individual measurement routes than the widely reported exponential and double exponential models. An heuristic explanation of the proposed autocorrelation property is also presented.**

I. Introduction

The performance of mobile radio systems is remarkably affected by fading phenomena. The envelope of the received signal transmitted through a radio channel will typically experience the fast and slow fading. The fast fading results from the superposition of randomly scattered multipath components. The slow fading, due to blockage from objects in the signal path, is also referred to as shadow fading. The most common model which had been empirically confirmed for slow fading is log-normal shadowing. The spatial autocorrelation behavior of the shadow fading process is important in many different fields in mobile communications, including the study of the quality of service in mobile systems, the design of handover procedure [1], [2], and the coverage of multi-hop cellular networks [3].

The spatial autocorrelation of shadow fading has been investigated in numerous studies. Many measurements have been taken by researchers to characterize the empirical autocorrelation function of the shadow fading process over distance for different environments at different frequencies [4]–[9]. The most commonly analytical model for the autocorrelation of shadow fading first proposed by Gudmundson [4] and based on empirical measurements. The shadowing was modeled as a first-order autoregressive process (AR(1)) which implies an exponential decaying autocorrelation function. Although it is currently widely adopted for the evaluation of radio transmission technologies [10], the model fit is good for suburban environment, while it gives poor results for urban environment [4]. Other measurements also reported this model fits the empirical results in typical urban and bad urban environments in Sweden [6], suburban environments in Finland [8], and a bridge-to-car hot-spot environment in Germany [9]. This model was improved later in [11] to avoid the inconsistencies with the level crossing theory when the Gudmundson model is been extending to continuous-space case. Besides the exponential decaying model, in [5], an autoregressive moving average model (ARMA(2,1)) is obtained by a combination of parametric system identification and classical spectral estimation procedures, based on the measured data in urban environment. The ARMA(2,1) model gives a double exponential decaying autocorrelation function. Coherence finding is reported in suburban macro environment in Denmark [6]. The AR(1) model is a special case of ARMA(2,1) model. The latter can neither be readily extended to the continuous-space case for the same reason as the AR(1) model. To avoid this problem, two heuristic models were proposed [12], [13] assuming the power spectral density (PSD) of the shadow fading process having the shape of the Gaussian function or the Butterworth filter, respectively. However, these two models have not been confirmed by any measurement. In the related literatures, the measurement campaigns were conducted in American and European countries. The autocorrelation of shadow fading based on measurements in China has not been reported yet.

In this paper, we present a novel empirical autocorrelation model for the shadow fading process, based on field measurements at 2.35 GHz in an urban area of a typical medium-sized Chinese city. The proposed models fit the measured data very well while revealing accordance with the level crossing theory of Gaussian process.

The outline of the remaining of the paper is as follows. The measurement campaign is described in Section II. The detailed processing procedure of the measured data is explained in Section III. The proposed autocorrelation model and its heuristic explanation is presented in Section IV. Section V concludes the whole paper.

II. Measurement Campaign

A. Measurement System and Antennas

Extensive channel measurements were performed at the center frequency of 2.35 GHz with 100 MHz bandwidth

978-1-4244-2324-8/08/$25.00 © 2008 IEEE.

This full text paper was peer reviewed at the direction of IEEE Communications Society subject matter experts for publication in the IEEE "GLOBECOM" 2008 proceedings.

(a) Picture of the ODA.

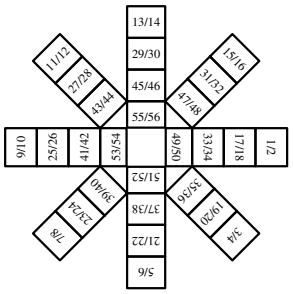

(b) Layout of the elements.

Fig. 1. 3×8 Omni-directional antenna array.

TABLE I
GENERAL SOUNDER PARAMETERS.

Items	Settings
Center frequency	2.35 GHz
Chip rate	100 MHz
Sampling rate	200 MHz
TX power at antenna input	40 dBm
PN code length	1023
Measurement cycle rate	436.4 Hz
No. of elements of RX array	56
Samples of IR per wavelength at 30 km/h	6.69

with Elektrobit Propsound™ CS channel sounder [14] in Shijiazhuang, China. A single vertical polarized dipole was employed at the transmitter (TX) as the base station (BS) antenna. As for the mobile station (MS), a three-dimensional dual-polarized ($\pm 45°$) omni-directional array (ODA) was used at the receiver (RX). There are 48 elements aligned in 3 rings and 8 elements on the top of the array as shown in Fig. 1. The element spacing of the ODA is half of a wavelength. The TX antenna is fixed on a mast on the rooftop of a 7-floor building. The RX antenna array is mounted on the top of a vehicle, which was driving at a speed of about 30 km/h. Summary of measurement parameters is listed in Table I. In the sequel, the label "SJZ-2G35" is utilized to identify this measurement campaign.

B. Environment

The measured environment is a typical urban area of a medium-sized Chinese city. It is characterized by buildings ranging from 4 to 12 floors and an regular street grid. During the measurement, the base station height was about 30 m which is well above the averaged height of the rooftop of the surrounding buildings. The mobile station height was about 2.5 m. Only very close to the BS there were clear line-of-sight (LOS) propagation condition. When the MS is getting further away, the MS and BS was obstructed mainly by buildings. In most cases, there was no LOS path between the BS and the MS. Measurements were performed along 17 routes as shown in Fig. 2 where the star denotes the location of the BS. The covered range of the measurements is about 1.5 km in radius.

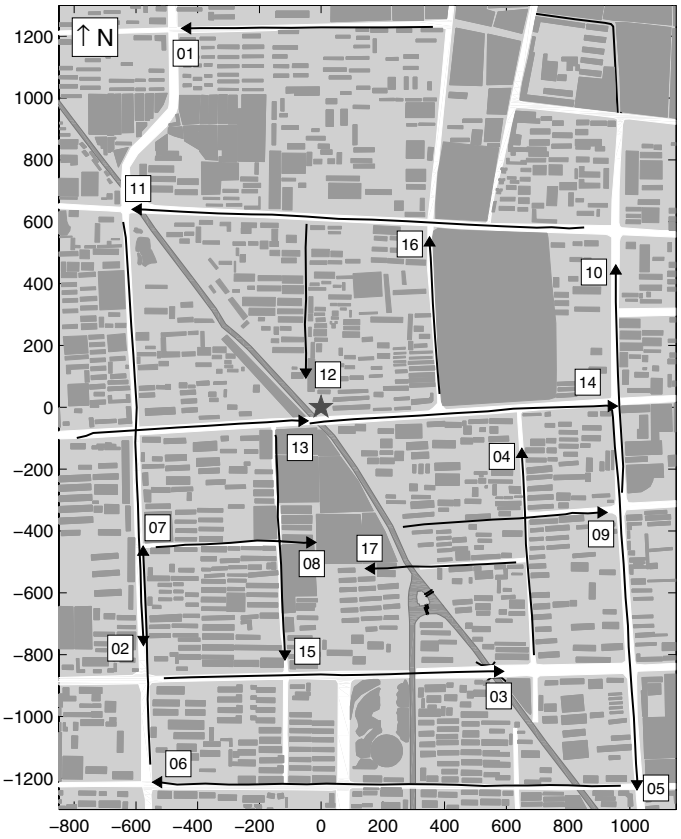

Fig. 2. Measured routes for SJZ-2G35. The axis ticks are in 1 m.

III. ANALYSIS OF MEASUREMENT DATA

A. Pre-selection

Firstly, the position of each measurement data point is extracted from the GPS records. The longitude-latitude coordinates are converted into 2D-Cartesian coordinates with the coordinates of TX as $(0, 0, \Delta z)$, here Δz is the difference between the height of both TX and RX. Let vector $\boldsymbol{r} = (x, y, 0)$ be the position of a measurement location. The data points with MS-BS distance less than 50 meters were precluded in the processing. This pre-selection ensures that the BS/MS antenna pattern does not dominate the analysis result [8].

B. Extraction of Shadow Fading Components

The measured channel impulse response between the TX and the mth RX element obtained by sliding correlation detector at position $\boldsymbol{r}$ can be modeled as

$$h'_m(\tau; \boldsymbol{r}) = 10^{[G-\xi(\boldsymbol{r})-L(\boldsymbol{r})]/20} \cdot h_m(\tau; \boldsymbol{r}), \qquad (1)$$

where G is the gain introduced by the sounder and the measurement antennas, $\xi(\boldsymbol{r})$ is a zero mean Gaussian process which causes the shadowing, $L(\boldsymbol{r})$ is the radio channel's path loss, all in decibels. $h_m(\tau; \boldsymbol{r})$ is the multipath component which causes the fast fading. Assume that the average power gain of the multipath component is unitary, i.e.,

$$\mathcal{E}_{\boldsymbol{r}} \left\{ \int |h_m(\tau; \boldsymbol{r})|^2 d\tau \right\} = 1, \qquad (2)$$

This full text paper was peer reviewed at the direction of IEEE Communications Society subject matter experts for publication in the IEEE "GLOBECOM" 2008 proceedings.

where $\mathcal{E}_{\boldsymbol{r}}\{\cdot\}$ stands for the expectation operation of $\boldsymbol{r}$. The received power over the mth sub-channel is given by

$$P_m(\boldsymbol{r}) = \int |h'_m(\tau;\boldsymbol{r})|^2 d\tau. \quad (3)$$

In order to estimate the shadow fading components, the fast fading component in $P_m(\boldsymbol{r})$ needs to be removed. Define the *local area* of position $\boldsymbol{r}$ as the circular range centered at position $\boldsymbol{r}$ with a constant radius R. Let $\mathcal{A}(\boldsymbol{r};R)$ be the set of measurement positions within the local area of position $\boldsymbol{r}$. Denote the received power at position $\boldsymbol{r}$ by $P(\boldsymbol{r})$ which is obtained by averaging over the ensemble $\{P_m(\boldsymbol{s}) : \boldsymbol{s} \in \mathcal{A}(\boldsymbol{r};R); m = 1,2,\ldots,56\}$. It is assumed that the fast fading is removed, so the received power in decibels approximates the summation of shadowing $\xi(\boldsymbol{r})$, path loss $L(\boldsymbol{r})$ and the gain G.

The single-slope log-distance model is adopted to estimate the distance dependent path loss, which is of the form

$$L(\boldsymbol{r}) = 10\gamma \log_{10} \|\boldsymbol{r}\|_2 + A, \quad (4)$$

where $\|\boldsymbol{r}\|_2$ is the MS-BS distance in meters, and A is the interception in decibel. Linear regression using a minimum mean square error (MMSE) criterion was utilized to estimate the parameter γ and the differences between G and A. The fitted path loss exponent $\gamma = 3.66$ and $G - A = -9.34$ dB. Thus, the shadowing component in decibel is given by

$$\xi(\boldsymbol{r}) = (G - A) - 10\gamma \log_{10} \|\boldsymbol{r}\|_2 - P(\boldsymbol{r}). \quad (5)$$

C. Normality Testing

Good agreement can be seen from the normal probability plot in Fig. 3. It shows that the extracted shadow fading samples formed an approximate straight line. So, the samples can be regarded as normally distributed. The t-test of the null hypothesis that the shadowing samples are from a zero mean normal distribution with unknown variance indicates a failure to reject the null hypothesis at the 1% significance level (the p-value of the test is 0.661). The histogram of the shadow fading samples is shown in Fig. 4. The standard deviation σ_ξ is 5.0 dB.

IV. Autocorrelation Function of the Shadow Fading

Denote all the extracted shadow fading samples by a set $\mathcal{S} = \{\xi_1, \xi_2, ..., \xi_S\}$. Let d_{ij} be the distance between the ith and the jth sample. Let $\mathcal{S}_q$ be a non-null subset of $\mathcal{S}$. For a given distance resolution Δd, the autocorrelation of shadow fading, $\rho(d)$, is estimated over set $\mathcal{S}_q$ at a series of discrete distances d_k as

$$\hat{\rho}(d_k) = \frac{\sum_{(i,j)\in\mathcal{I}_k} (\xi_i - \mu_{k1})(\xi_j - \mu_{k2})}{\sqrt{\sum_{(i,j)\in\mathcal{I}_k} (\xi_i - \mu_{k1})^2} \cdot \sqrt{\sum_{(i,j)\in\mathcal{I}_k} (\xi_j - \mu_{k2})^2}}, \quad (6)$$

where $d_k = k\Delta d, k \in \mathbb{Z}$, and

$$\mathcal{I}_k = \left\{ (i,j) : (d_{ij} - k\Delta d) \in \left[-\frac{\Delta d}{2}, +\frac{\Delta d}{2} \right); \xi_i, \xi_j \in \mathcal{S}_q \right\}. \quad (7)$$

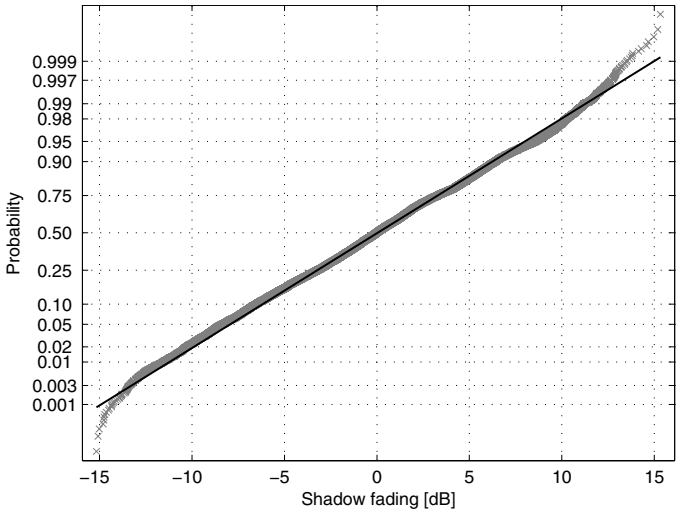

Fig. 3. Normal probability plot of shadow fading empirical distribution function (EDF).

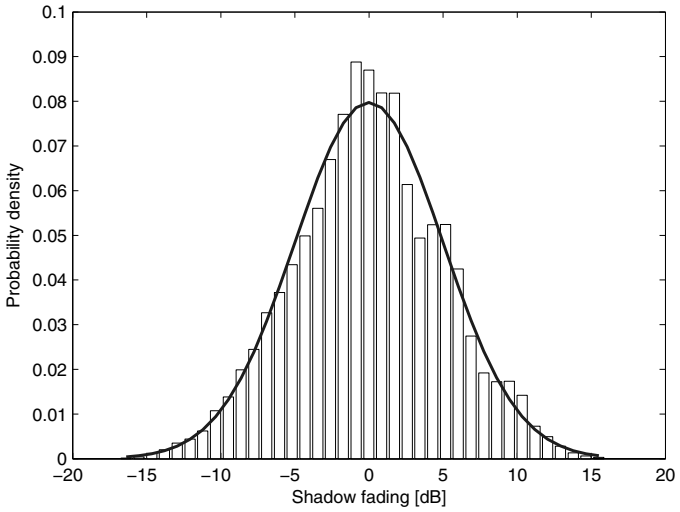

Fig. 4. Shadow fading distribution with a normal fit (solid line).

In (6), μ_{k1} and μ_{k2} are the sample means of the sets $\{\xi_i : \xi_i \in \mathcal{S}; (i,j) \in \mathcal{I}_k\}$ and $\{\xi_j : \xi_j \in \mathcal{S}; (i,j) \in \mathcal{I}_k\}$, respectively. We choose the distance resolution to be about 20 wavelengths, i.e. $\Delta d = 2.5$ m.

A. The Double Exponential Model

When choosing $\mathcal{S}_q = \mathcal{S}$, namely, all shadow fading samples extracted from all measured routes, the estimated autocorrelation is plotted in Fig. 5. The double exponential model [5], [6]

$$\rho(d) = \alpha \exp\left(-\frac{|d|}{D_1}\right) + (1-\alpha)\exp\left(-\frac{|d|}{D_2}\right), \quad (8)$$

fits the measured data in SJZ-2G35 as shown in Fig. 5 with $D_1 = 2.3$ m, $D_2 = 121$ m, and $\alpha = 0.2$. The correlation at distance 58 m was estimated to be 0.5.

This full text paper was peer reviewed at the direction of IEEE Communications Society subject matter experts for publication in the IEEE "GLOBECOM" 2008 proceedings.

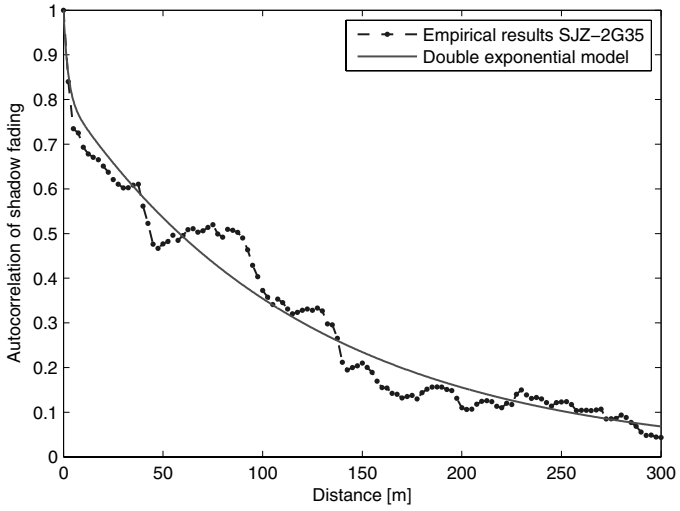

Fig. 5. Empirical spatial autocorrelation function of shadow fading in SJZ-2G35. A double exponential model is matched to the empirical results.

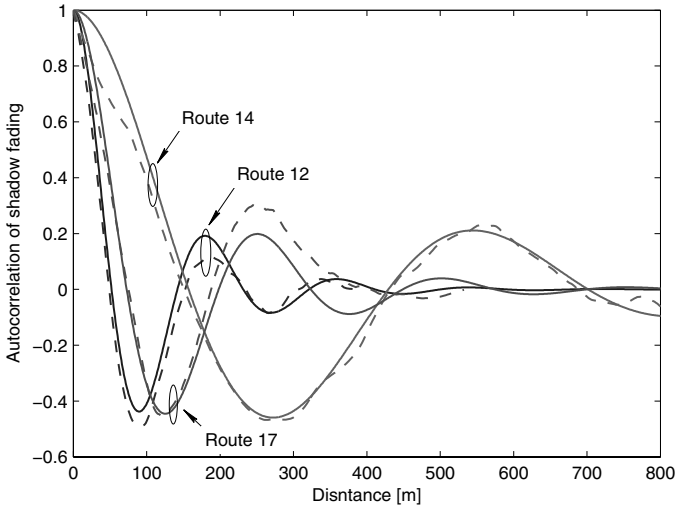

Fig. 6. Empirical spatial autocorrelation functions of shadow fading of several single routes in SJZ-2G35. The proposed exponential decaying sinusoid model provides good matches to the empirical results. The dashed lines are empirical results, while the solid lines are the fitted curves.

B. Exponential Decaying Sinusoid Model

When choosing $\mathcal{S}_q$ to be the shadowing samples extracted from a single route, the estimated autocorrelation is very different from the exponential decaying model or the double exponential model. Fig. 6 shows examples of empirical autocorrelation of shadow fading of some routes in SJZ-2G35 (solid lines). By visual inspection, we propose the autocorrelation as an *exponential decaying sinusoid* function,

$$\rho(d) = \frac{1}{\cos c_3} \exp(-c_1|d|)\cos(c_2|d| + c_3), \tag{9}$$

where $c_1 > 0$, $c_2 \neq 0$, $c_3 \neq (n - 1/2)\pi$, $n \in \mathbb{Z}$. Further, consider the level-crossing theory, the level crossing rate (LCR) of a zero-mean continuous-space Gaussian process with autocorrelation $\rho(d)$ is a function of the second derivative $\rho''(0)$ [11]. Consequently, the parameters $\{c_1, c_2, c_3\}$ need to be constrained by

$$c_1 + c_2 \tan c_3 = 0, \tag{10}$$

such that the underlying autocorrelation function in (9) is twice differentiable at the origin. The detailed derivation of (10) is given in the Appendix. With this constraint, the autocorrelation function in (9) can be rewritten as

$$\rho(d) = \exp\left(-\frac{|d|}{D_3}\right)\left[\cos\left(\frac{|d|}{D_4}\right) + \frac{D_4}{D_3}\sin\left(\frac{|d|}{D_4}\right)\right], \tag{11}$$

where $D_3 > 0$, $D_4 > 0$. The second derivative at zero is given by

$$\rho''(0) = -\frac{D_3^2 + D_4^2}{D_3^2 D_4^2}. \tag{12}$$

As shown in Fig. 6, the proposed model fits the measured autocorrelation very well for distances up to 200 m for all three routes. Particularly, the model works "satisfactorily" for Route 14 for distances up to even 800 m. The fitted parameters are summarized in Table II, where $d_{0.5}$ is the decorrelation distance, namely, the minimum distance where the correlation equals to 0.5. It shows that the decorrelation distance $d_{0.5}$ varies for different routes where different propagation environments are experienced. The differences among these routes include the width of the road, the height and the extent of buildings along the road. A rough comparison on these factors is that the width of the road and the extent of buildings of Route 14 is greater than the values of Route 17, and further greater than the values of Route 12, while the decorrelation distance decreases sequentially.

TABLE II
FITTED PARAMETERS OF THE EXPONENTIAL DECAYING SINUSOID AUTOCORRELATION MODEL FOR SELECTED ROUTES IN SJZ-2G35.

Parameters	Route 12	Route 17	Route 14
D_3 [m]	109	155	350
D_4 [m]	29	40	87
$d_{0.5}$ [m]	32	45	97

C. Heuristic Explanation

A heuristic explanation to the autocorrelation property in form of such exponential decaying sinusoid is that an urban area can be virtually divided into several blocks by the roads and the buildings. The shadow fading within a *virtual block* (VB) are correlated while the decorrelation distance depends on the size of the VB. Larger extent of the buildings and wider roads lead to VBs in larger size. As a consequence, longer decorrelation distance is yielded. The shadowing in the center of a VB can be quite different from the shadowing at the boundary of adjacent VBs, this could be the reason for the negative correlation values. There can be some similarity between adjacent VBs. Consider that the MS is moving from one VB to another by passing a virtual boundary, the correlation of shadow fading decreases when it's moving out

This full text paper was peer reviewed at the direction of IEEE Communications Society subject matter experts for publication in the IEEE "GLOBECOM" 2008 proceedings.

a VB and entering the virtual boundary; then the correlation increases during its entering to the adjacent VB which is similar to the previous one. The exponential or double exponential correlation property can be thought as certain average of the exponential decaying sinusoid correlation property over all individual routes in an environment.

V. Conclusion

In this paper, the spatial autocorrelation of shadow fading in the urban environment in a typical Chinese city with medium size is investigated. A novel autocorrelation model is proposed based on the measured data. It reveals accordance with the level crossing rate theory of Gaussian processes. The proposed model provide better match to the empirical results of individual routes, while the double exponential model gives an overall description of the autocorrelation of shadow fading of the entire environment. A heuristic explanation of the exponential decaying sinusoid autocorrelation property is also suggested.

Appendix

This appendix is devoted to the derivation of the (10). The necessary condition for that $\rho(x)$ is twice differentiable at zero is that the first derivative of $\rho(x)$ exists at zero. According to the definition of derivative, we have

$$\rho'_+(0) = \rho'_-(0), \tag{13}$$

where both $\rho'_+(0)$ and $\rho'_-(0)$ are one-sided limit:

$$\rho'_+(0) = \lim_{h\to 0^+} \frac{\rho(h)-\rho(0)}{h}, \tag{14}$$

$$\rho'_-(0) = \lim_{h\to 0^-} \frac{\rho(h)-\rho(0)}{h}. \tag{15}$$

Substitute (9) in (14) and (15), then with (13) it yields the equality (10).

Then, investigate whether $\rho(x)$ is twice differentiable at zero under the condition (10). When such condition holds, the derivative of $\rho(x)$ can be found as

$$\rho'(x) = -\frac{c_2^2}{\cos^2 c_3} x \exp(c_2|x|\tan c_3)\,\mathrm{sinc}(c_2|x|), \tag{16}$$

where $c_3 \neq (n-1/2)\pi, n \in \mathbb{Z}$. Again, using the definition of derivative, the second derivate of $\rho(x)$ at zero is obtained

$$\rho''(0) = -\frac{c_2^2}{\cos^2 c_3}. \tag{17}$$

Thus, the function $\rho(x)$ in (11) is second differentiable at zero.

Acknowledgment

This work was supported in part by the National 863 High Technology Research and Development Program of China under Grant No. 2006AA01Z258, and by Research Institute of China Mobile Communications Corporation.

References

[1] F. Santucci, M. Pratesi, M. Ruggieri, and F. Graziosi, "A general analysis of signal strength handover algorithms with cochannel interference," *IEEE Trans. Commun.*, vol. 48, no. 2, pp. 231–241, Feb. 2000.

[2] H.-P. Lin, R.-T. Juang, and D.-B. Lin, "Validation of an improved location-based handover algorithm using GSM measurement data," *IEEE Trans. Mobile Comput.*, vol. 4, no. 5, pp. 530–536, Sep.–Oct. 2005.

[3] K. Yamamoto, A. Kusuda, and S. Yoshida, "Impact of shadowing correlation on coverage of multihop cellular systems," in *Proc. 2006 IEEE International Conference on Communications (ICC'06)*, vol. 10, Istanbul, Turkey, Jun. 11–15, 2006, pp. 4538–4542.

[4] M. Gudmundson, "Correlation model for shadow fading in mobile radio systems," *Electronics Letters*, vol. 27, no. 23, pp. 2145–2146, Nov. 1991.

[5] T. B. Sørensen, "Correlation model for slow fading in a small urban macro cell," in *Proc. 9th IEEE International Symposium on Personal, Indoor and Mobile Radio Communications (PIMRC'98)*, vol. 3, Boston, USA, 1998, pp. 1161–1165.

[6] A. Algans, K. I. Pedersen, and P. E. Mogensen, "Experimental analysis of the joint statistical properties of azimuth spread, delay spread, and shadow fading," *IEEE J. Sel. Areas Commun.*, vol. 20, no. 3, pp. 523–531, Apr. 2002.

[7] J. Weitzen and T. J. Lowe, "Measurement of angular and distance correlation properties of log-normal shadowing at 1900 MHz and its application to design of PCS systems," *IEEE Trans. Veh. Technol.*, vol. 51, no. 2, pp. 265–273, Mar. 2002.

[8] T. Rautiainen, K. Kalliola, and J. Juntunen, "Wideband radio propagation characteristics at 5.3 GHz in suburban environments," in *Proc. 16th IEEE International Symposium on Personal, Indoor and Mobile Radio Communications (PIMRC'05)*, Berlin, Germany, Sep. 11–14, 2005, pp. 868–872.

[9] A. Hong, M. Narandzic, C. Schneider, and R. S. Thomä, "Estimation of the correlation properties of large scale parameters from measurement data," in *Proc. IEEE 18th International Symposium on Personal, Indoor and Mobile Radio Communications (PIMRC'07)*, Athens, Greek, Sep. 3–7, 2007, pp. 1–5.

[10] "Selection procedures for the choice of radio transmission technologies of the UMTS (UMTS 30.03), v3.2.0," ETSI, 1998.

[11] D. Giancristofaro, "Correlation model for shadow fading in mobile radio channels," *Electronics Letters*, vol. 32, no. 11, pp. 958–959, May 1996.

[12] M. Pätzold, U. Killat, and F. Laue, "An extended Suzuki model for land mobile satellite channels and its statistical properties," *IEEE Trans. Veh. Technol.*, vol. 47, no. 2, pp. 617–630, May 1998.

[13] M. Pätzold and K. Yang, "An exact solution for the level-crossing rate of shadow fading processes modelled by using the sum-of-sinusoids principle," in *Proc. 9th International Symposium on Wireless Personal Multimedia Communications (WPMC'06)*, San Diego, USA, Sep. 17–26, 2006, pp. 188–193.

[14] Elektrobit, "Propsound CS: The ultimate technology in radio propagation measurement." [Online]. Available: http://www.propsim.com/file.php?732